KCNQ1 and KCNE1 K+ Channel Components are Involved in Early Left-Right Patterning in *Xenopus laevis* Embryos

Junji Morokuma, **Douglas Blackiston**, and **Michael Levin**
Center for Regenerative and Developmental Biology, Forsyth Institute, and Developmental Biology Department, Harvard School of Dental Medicine 140 The Fenway Boston

Abstract

Several ion transporters have been implicated in left-right (LR) patterning. Here, we characterize a new component of the early bioelectrical circuit: the potassium channel KCNQ1 and its accessory subunit KCNE1. Having cloned the native *Xenopus* versions of both genes, we show that both are asymmetrically localized as maternal proteins during the first few cleavages of frog embryo development in a process dependent on microtubule and actin organization. Molecular loss-of-function using dominant negative constructs demonstrates that both gene products are required for normal LR asymmetry. We propose a model whereby these channels provide an exit path for K^+ ions brought in by the H^+,K^+-ATPase. This physiological module thus allows the obligate but electroneutral H^+,K^+-ATPase to generate an asymmetric voltage gradient on the left and right sides. Our data reveal a new, bioelectrical component of the mechanisms patterning a large-scale axis in vertebrate embryogenesis.

Keywords

KCNQ1; KCNE1; Potassium channel; Left-right asymmetry; *Xenopus*

Introduction

Bioelectric controls of embryonic patterning

Most modern work on developmental biology focuses on biochemical signals that control morphogenesis. However, a large body of research indicates that physical parameters, such as ion fluxes and endogenous voltage gradients, control crucial aspects of cell behavior [1-3]. Roles for bioelectric signals have been uncovered in galvanotaxis of migratory cell types including neural crest, wound healing, limb development, and mitotic control (reviewed in [4-6]). One context in which ion transporter activity couples to large-scale pattern formation is in left-right (LR) patterning.

Vertebrates, and many invertebrates, possess a bodyplan that is basically bilaterally symmetrical, with the striking exception of the consistent placement of the heart and viscera, as well as lateralization of the brain [7, 8]. The embryonic generation of asymmetry is now understood to involve conserved independent left- and right-sided cascades of asymmetric gene expression feeding into the asymmetric morphogenesis of individual organs [9, 10]. Recent work revealed that in several species, physiological asymmetries in voltage, pH, and

Michael Levin, Center for Regenerative and Developmental Biology, Forsyth Institute, and Developmental Biology Department, Harvard School of Dental Medicine, 140 The Fenway, Boston MA 02115 (USA), Tel. +1 617 892-8403, Fax +1 617 892-8597, mlevin@forsyth.org.

intracellular small molecule movement control LR patterning at the very earliest stages of development (upstream of asymmetric gene expression) [11-13].

Ion transporters' roles in left-right asymmetry

Seeking to identify the transporters responsible for the asymmetry-relevant ion flows, Levin et al. performed a screen in *Xenopus* [14] which implicated three transporters: the H^+/K^+-ATPase exchanger [13], the V-ATPase H^+ pump [15], and a K^+ inward rectifier [16]. Using loss- and gain-of-function (by misexpression of mRNAs encoding wild-type and dominant-negative constructs), characterization of embryonic and subcellular localization of native maternal proteins, and physiological measurements of ion flux and transmembrane voltage, several of these transporters were functionally validated as obligate components of LR patterning long before ciliogenesis.

The three implicated transporters are present as maternal proteins in the egg. During the first few cleavages (which establish the prospective midline axis [17, 18]), they are transported in to one side of the midline [19], accumulating in one of the cells. This consistently asymmetric localization gives rise to a directly measurble oriented asymmetry in H^+ efflux and membrane voltage difference between the ventral blastomeres. When these physiological asymmetries are experimentally equalized, asymmetric gene expression and *situs* of the heart, gut, and gall-bladder are randomized in the absence of other defects (including those of dorso-anterior development).

Quantitative models are currently being built which attempt to synthesize the phenomena beginning with asymmetric localization of channels and pumps within early cells, leading to asymmetric voltage gradients, affecting in turn movement of small molecule morphogens through gap junction paths [20, 21], and ultimately leading to stabilization of asymmetric gene expression. However, one major piece remains unknown.

By itself, the H^+,K^+-ATPase (which is the best-understood component of this system) is electroneutral, exchanging two positive charges in each cycle [22]. Thus, it is entirely unclear how the asymmetric activity of this pump results in the measured membrane voltage difference across the ventral midline. However, the initial screen also implicated the KCNQ1 K^+ channel, which could in principle support the exit of the K^+ ions brought in by the H^+,K^+-ATPase, thus allowing a net loss of positive ions. Such a scheme could allow the two transporters, when working together, to alter membrane voltage levels. Interestingly, precisely this cooperative functional relationship is known to exist between the H,K-ATPase and KCNQ1 in a several mammalian tissues [23-29].

KCNQ1 and KCNE1 channels

KCNQ1 (also known as KvLQT1) is a 6-transmembrane member of the K^+ channel family (Fig. 5). When co-assembled with KCNE1 (a.k.a. minK, IsK), it forms the "slow delayed rectifier" or I_{Ks} channel [30]. Coexpression of KCNE1 alters the biophysical channel features of KCNQ1 by shifting the voltage dependence, slowing activation kinetics, abolishing inactivation, and increasing the single-channel conductance and the current amplitude [31]. KCNQ1 has different pharmacological profiles depending on whether it is associated with KCNE1 [32, 33].

KCNQ1 has a number of important biological roles, being responsible for an inherited birth defect that leads to cardiac arrhythmia - the so-called long-QT syndrome [28, 32, 34-38], and for the hearing loss observed in Jervell and Lange-Nielsen Syndromes [39, 40]. The KCNQ1 channel is also required for gastric acid secretion, where it works together with the H^+/K^+-ATPase [26, 28, 29]. It is thought that the KCNQ1 plays a crucial role in luminal K^+ recycling during the acid secretion necessary for normal digestion [27]. It appears that the

KCNE1 subunits do not play a role in modulation of the pH gradient produced by H^+/K^+-ATPase activity because the KCNE1 knockout mouse has normal acid secretion [29].

Thus, in order to fully understand the bioelectrical circuit responsible for physiological LR asymmetries, we focused on embryonic functions of KCNQ1 in the *Xenopus* embryo. Our expression and functional analysis reveals an endogenous role for this protein in left-right patterning.

Materials and Methods

Animal husbandry

Xenopus embryos were collected according to standard protocols [41] in 0.1X Modified Marc's Ringers (MMR) pH 7.8 + 0.1% Gentamicin. *Xenopus* embryos were staged according to [42].

Chromogenic in situ hybridization

In situ hybridization was performed according as previously described [43]. *Xenopus* embryos were collected and fixed in MEMFA. Prior to in situ hybridization, embryos were washed in PBS + 0.1% Tween-20 and then transferred to methanol through a 25%/50%/75% series. Probes for in situ hybridization were generated in vitro from linearized templates using DIG labeling mix from Invitrogen. Chromogenic reaction times were optimized for signal: background ratio. Marker analyses were done on 70-80 embryos for each marker.

Xenopus Microinjection

For microinjections, capped, synthetic mRNAs [41] were dissolved in water and injected into embryos in 3% Ficoll using standard methods (50-150 msec pulses in each injected cell with borosilicate glass needles calibrated for a bubble pressure of 50-70 kPa in water). Injections delivered approximately 2.7 nL into each cell. After 30 minutes embryos were washed in 0.75X MMR for 30 minutes and cultured in 0.1X MMR until desired stages. Results of injections are reported as: % of otherwise normal embryos that were heterotaxic, sample size (N), and χ^2 and p values comparing treated to controls (using Pearson correction).

Immunohistochemistry

Embryos were fixed overnight in MEMFA and stored at 4 °C in PBTr (1X PBS + 0.1% Triton-100). They were embedded in gelatin/albumin medium, and sectioned at 40 μ on a Leica vibratome as previously described [44]. The sections were then washed 3X in PBTr, blocked with 10% goat serum, and incubated with primary antibody at 1:500 in PBTr overnight, washed 6X with PBTr, and incubated with an alkaline-phosphatase-conjugated secondary antibody overnight. After 6 washes in PBTr, detection was carried out using NBT and BCIP (X-Phos). Chromogenic reaction times were optimized for signal: noise ratio. Antibodies used were: a polyclonal antibody to IsK [45] used at 1:1000, and two KCNQ1 antibodies generated by Invitrogen to peptide sequences TYEQLNVPRMTQDNIS and ITHISELKEHHRAAIK (used at 1:500). Consensus patterns are reported for each plane of section and embryonic stage based on N>20.

Drug exposure

KCNQ blockers (obtained from Sigma and Tocris) were made as 1000X aliquots in DMSO, and used as: Chromanol293B - 300 μM [46, 47], Clofilium tosylate - 100 μM [48], L-768673 – 90 μM [49], Linopiridine – 5 mM) [50], RL-3 – 10 μM [51].

Cytoskeleton modulating compounds (Molecular Probes): the microtubule disruptor Nocodazole [52, 53] and the microfilament disruptor Latrunculin [54, 55] were used at 50 nM and 4 μM respectively.

Laterality assay

Xenopus embryos at st. 45 were analyzed for position (*situs*) of 3 organs: the heart, stomach, and gallbladder [56]. Heterotaxia was defined as reversal in one or more organs. Only embryos with normal dorsoanterior development (DAI=5) were scored, thus avoiding confounding randomization caused by midline defects [57], and clear left- or right-sided organs were scored; percent heterotaxia was calculated as number heterotaxic divided by the number of total scorable embryos, i.e. embryos normal in all other ways, with DAI=5. A χ^2 test (with Pearson correction for increased stringency) was used to compare absolute counts of heterotaxic embryos.

Western blotting

Twenty-five *Xenopus* embryos at the 4-cell stage were resuspended in lysis buffer (1% Triton X100, 50 mM NaCl, 10 mM NaF, 1 mM Na_3VO_4, 5 mM EDTA, 10 mM Tris pH 7.6, 2 mM PMSF). Protein solution was mixed at 1:1 with Laemmli sample buffer (Biorad) containing 2.5% 2-mercaptoethanol. The proteins were fractionated by SDS-PAGE and electrotransferred to a PVDF membrane. After washing, the membrane was blocked with 3% bovine serum albumin and 5% dry milk in tris-buffered saline including 0.1% Tween-20. It was then incubated overnight in a Mini-PROTEAN II multiscreen apparatus (Biorad) at 4 °C with the primary antibody, diluted in TTBS + 3% BSA + 5% dry milk. After washing, the blots were incubated with peroxidase-conjugated second antibody (1:5000) and developed using an ImmunoStar Chemiluminescent Protein Detection System (Biorad) according to the manufacturer's instructions.

Cloning and plasmid construction of Xenopus laevis KCNQ1 and KCNE1

Xenopus laevis full length xKCNQ1 cDNA was isolated from Yamamoto/Hyodo-Miura NIBB/NBRP Xenopus DMZ library-derived ESTs, utilizing the known partial sequence (Genbank accession #U71076, [58]) against the EST database XDB (http://Xenopus.nibb.ac.jp). Candidate EST clone XL240i21ex was fully sequenced, and by open reading frame prediction, and by also multiple sequence alignment analysis using Clustal W software, was seen to contain the complete coding region of xKCNQ1 (Genbank accession #EF078696). The plasmid clone was named pCS2p+xKCNQ1. In order to remove the 3′-UTR region from pCS2p+xKCNQ1, primers xKCNQ1-ORF-Up [5′-AGA TAT ATT GTC CTG AGT CAT CCT CGG CAC-3′] and pCS2p+Stop+XhoI-Down [5′-TGA CTC GAG CCT CTA GAT TCT GCA GCC CTA-3′] were used in PCR mutagenesis by KOD Hot Start DNA polymerase (Novagen, Madison, WI), constructing pCS2p+xKCNQ1_ORF. A constitutively-active (CA) mutation based on homologous human mutation (hKCNQ1_S140G, [59] was introduced into pCS2p+xKCNQ1_ORF by KOD Hot Start PCR mutagenesis using primers xQ1_S130G mut-down [5′-GAG TAC TTT CTA CAA TAC AGC AGT ATA ACA-3′] and xQ1_S130G mut-up [5′-CGA AGA TCA GAC ATA TCA ACA CGA TGA GGA-3′], constructing pxQ1_S130G(CA). In a similar manner, a homologous dominant-negative (DN) mutation (hKCNQ1_V254M, [34, 60, 61], was introduced using primers xQ1_V244M down [5′-TGG TTT TTA TTC ATA GAC AAG AAC TGA TCA-3′] and xQ1_V244M mut-up [5′-TGG ATC CGA GTA ATC TCC ATG TGC CGC CTG-3′], constructing pxQ1_v244M(DN). Similarly, homologous ER-retained dominant-negative (ER-DN) mutations (hKCNQ1_ Y111C & _L114P, [62]) were introduced using primers xQ1_Y101C down [5′-CAA CTT CTT AGA GCG GCC CAC CGG CTG GAA-3′] and xQ1_Y101C mut-up [5′-CAA ACT CTG CCC TGG ATG TTG GTC CGG CTG-3′] to construct pxQ1_Y101C (ER-DN), and primers xQ1_L104P mut-

down [5′-CAG AGC GGC CCA CCG GCT GGA AAT GCT TCG-3′] and xQ1_L104P mut-up [5′-GGA AGT TGT AAA CTC TGC CCT GGA TGT TGG-3′] to constructpxQ1_L104P (ER-DN). Double-DN mutants pxQ1_Y101C+V244M and pxQ1_L104P+V244M were constructed in parallel, using pxQ1_v244M(DN) as template.

Full length xKCNE1 cDNA was cloned from stage 25 embryo cDNA by PCR using primers xKCNE1-Down5′ [5′-GGG AAT TCG TAG AAG GAG TCC AAG ATA GAG AAG AA-3′] and xKCNE1-Up3′ [5′-AGC TCG AGT CAG TTG CTG GGA GAA GAG GGG ATA TA-3′], designed from existing *Xenopus* laevis full length clone (Genbank accession #AF545500, [63]), and was subcloned into pCS2p+ vector's EcoRI-XhoI site, constructing pCS2p+xKCNE1. A homologous dominant-negative (DN) mutation (hKCNE1_G52R, [64]) was introduced using primers xE1_G46R down [5′-GAT TCT TCG GCT TTT TTA CTT TTG GGA TAA-3′] and xE1_G46R mut-up [5′-GCA GCA GTA GAA GGA TAT ACA CCA CTT CCA-3′], constructing pxE1_G46R(DN). Nucleotide sequences were confirmed by DNA sequencing.

β-gal staining

Embryos were fixed with MEMFA for 15 minutes at 4 °C and processed for β-gal staining using standard methods [41] using X-gal or Red-gal substrate.

Results

XKCNQ1 and XKCNE1 are implicated by a loss-of-function drug screen

A comprehensive hierarchical inverse drug screen was performed as previously described [14]. This strategy seeks to identify specific ion transporters functioning in laterality determination by successive application of increasingly-specific blocker compounds to embryos between fertilization and st. 8 (prior to gastrulation). The assay was specific reversals of one or more of the heart, gut, or gall bladder (heterotaxia) in the absence of other defects, generalized toxicity, or changes in dorsoanterior index [57, 65, 66]. This technique was previously used to identify roles in asymmetry for the serotonin pathway [12, 67] and for two specific H^+ and K^+ exchangers [11].

The results are summarized in Fig. 1A. As we previously reported [13, 15], most drug inhibitors targeting ion transporters had no effect on LR asymmetry. In particular, a variety of H^+ channels, Ca^{++} channels, voltage-gated Na^+ channels, Na^+/H^+ exchangers, and Ca^{++}-activated K^+ channels were revealed as very low-priority targets and not pursued further. Similarly, embryos treated with vehicle only exhibited the normal 1% background of heterotaxia. These data represent the negative controls; a positive control was the H^+/K^+-ATPase, which we characterized in previous work and which, when inhibited, resulted in ~50% randomization of the embryos.

Exposure of frog embryos (Table 1) from fertilization to st. 8 to barium chloride resulted in a significant degree of randomization (68%, p<<0.01) suggesting involvement of some kind of potassium conductance. A second round of the screen using more specific K^+ channel inhibitors revealed that exposure to the KCNQ blockers Chromanol293B [46, 47], Clofilium tosylate [48], L-768673 [49], and Linopiridine [50] induce significant rates of heterotaxia (Fig. 1A, columns marked with asterisk). Although the pharmacology by itself cannot prove a functional role, these data suggest KCNQ1 (Fig. 1B,C) as a possible channel involved in early embryonic asymmetry. Thus, we pursued the functional roles of this channel in early embryogenesis by generating mutations in native frog KCNQ1 and KCNE1 matching a series of characterized mutants recovered from human patients with long QT syndrome.

Cloning of native frog KCNQ1 and KCNE1

KCNQ1 is an ancient potassium channel, and has been described in *Drosophila* [68, 69] and *C.* elegans [70]. Full-length clones for XKCNQ1 (EF078696) and XKCNE1 (AF545500) were recovered from *Xenopus* laevis cDNA libraries as described in Materials and Methods. These α and β subunits exhibited 62%/78% and 54%/42% homology to the human sequence at the nucleotide/amino acid level respectively.

XKCNQ1 and XKCNE1 are required for normal LR asymmetry: molecular validation

We tested the hypothesis that XKCNQ1 and/or XKCNE1 are required for normal LR asymmetry by examining laterality in embryos expressing mutated subunits that are known to function in a dominant negative manner (by assembling with wild-type subunits and down-regulating endogenous complex function). Embryos at the 1-cell stage were injected with synthetic mRNA encoding dominant-negative XKCNQ1 proteins (Fig. 1D) that had been identified in human cardiac patients and characterized physiologically in *Xenopus* oocyte systems, allowed to develop to organogenesis stages, and then were analyzed for the positions of the heart, gut, and gall-bladder. Uninjected embryos, or embryos injected with β-gal or dominant negative Kir2.1 mRNA (negative control) only exhibited the low background level of heterotaxia (<4%). We generated a mutant of the native *Xenopus* sequence, with a valine 244 to methionine change in the cytosolic loop connecting the S4 and S5 transmembrane domain, matching the human dominant negative mutant V254M [61, 71]. This construct, as well as the ER-retention dominant negative mutant L104P [62], and the double mutant L104P+V244M, all caused significant levels of heterotaxia (p<<0.01, Table 2A). We conclude that the activity of XKCNQ1 is necessary for normal LR patterning (although our data do not rule out involvement of other K^+ channels). Overexpression of wild-type XKCNQ1 or of the S130G constitutively-active mutation of XKCNQ1 [59, 72] did not induce heterotaxia (2%, N=969), suggesting that XKCNQ1 is already activated under basal conditions during LR patterning.

Because adding the ER mutation to the V244M mutant increases the incidence of phenotype (a synergistic, additive effect), it is likely that the ER mutation does function as a dominant negative as previously described [62], and is not due to a cryptic gain-of-function effect of increased ion transport in the endoplasmic reticulum. The dominant negative mutant of XKCNE1, G46R (a mutation in the transmembrane domain that reduces the channel complex's current to about half of its normal value [64]), also caused significant levels of heterotaxia (p<<0.01, Table 2A). Thus, it is likely that XKCNE1 is required for LR patterning, and that the dominant negative construct acts by impairing endogenous XKCNQ1-XKCNE1 complex function.

We next examined the consequences of overexpression of the XKCNE1 accessory subunit (Table 2B). Microinjection of native *Xenopus* KCNE1 mRNA at the 1 cell (which distributes the protein throughout the embryo) resulted in 18% heterotaxia (p<<0.01). In light of the heterotaxia induced by both over- and under-expression of exogenous XKCNE1 mRNA throughout the embryo, we conclude that correct LR patterning requires a specific level and/or spatial distribution of native XKCNE1. In contrast, over-expression of wild-type XKCNQ1 or a constitutively-active form of XKCNQ1, or exposure to the KCNQ1 activator RL-3 [51] resulted in no significant heterotaxia (1-2%, N>100 in each case).

XKCNQ1 and XKCNE1 are expressed in embryos and asymmetrically localized at cleavage stages

To further characterize the roles of KCNQ1 and KCNE1 in embryonic patterning we determined the expression of these two channel components at the mRNA and the protein levels. We first performed *in situ* hybridization of embryos and sections with an antisense

probe for XKCNQ1. Maternal KCNQ1 mRNA is present in the egg prior to fertilization (Fig. 2A,B), and was detected during cleavage stages (Fig. 2C) but had disappeared by gastrulation Fig. 2D). Zygotic expression of KCNQ1 was characterized and will be reported elsewhere (forthcoming).

Since, at early stages (cleavage prior to MBT), maternal proteins often possess a localization that may not match mRNA, we next used immunohistochemistry to ascertain protein presence. Western blotting revealed that the antibody we generated to a peptide in the native *Xenopus* sequence was specific for KCNQ1, giving one clean band of the expected size (Fig. 3A; signal disappeared completely when excess blocking peptide was first incubated with antibody). At the 2-cell stage, the stain was present at the cell surface of just one cell (Fig. 3B-D), and by the time the dorso-ventral and LR axes could be ascertained (4-cell stage), this was revealed to be the right ventral cell (Fig. 3E). Examination of protein in the epidermis during tailbud stages (Fig. 3F) revealed the predicted cell-membrane localization for this channel protein (Fig. 3G).

We next performed *in situ* hybridization of embryos and sections with an antisense probe for XKCNE1. Maternal XKCNE1 mRNA was detected in the egg prior to fertilization and in cleavage-stage embryos (Fig. 4A-D). The XKCNE1 antibody [45] recognizes a single band of the correct size on Western blots (Fig. 5A). At the protein level, XKCNE1 is localized asymmetrically at the first two cleavages, but was seen to be left-sided as well as right-sided (Fig. 5B-G) in a population of embryos. Unlike XKCNQ1, there was not a consistent asymmetry in its sidedness. We conclude that both XKCNQ1 and XKCNE1 are present and asymmetrically localized at the very earliest stages of embryonic development, consistent with possible roles in LR patterning.

Asymmetric localization of XKCNQ1 and XKCNE1 is driven by cytoskeletal organization

The cytoskeleton is a key component of ion transporter localization in epithelia [74-76] and specifically in LR patterning [15, 19, 77]. Thus, we asked whether the localization of XKCNE1 along the animal-vegetal or left-right axes was likewise dependent on microtubule or actin organization by treating early embryos with low doses of cytoskeletal disruptoirs (which is sufficient to specifically randomize left-right patterning [19]) and then assaying XKCNE1 or XKCNQ1 protein distribution in immunohistochemistry on blastomere sections at the 2-4 cell stages. Disruption of microtubules with Nocodozole abolished the normal asymmetric pattern of XKCNE1 localization (Fig. 6A,B) as well as diminishing the normally clear restriction of the XKCNE1 protein to the vegetal half of the early blastomeres (Fig. 6D,E). Disruption of actin structure with Latrunculin likewise alters the pattern, resulting in a tight central bolus of protein instead of the normal distribution throughout the vegetal half (Fig. 6D,F). Similarly, XKCNQ1 protein, which is normally present at the animal pole (Fig. 6G), becomes largely vegetally-localized after disruption of actin structure with Latrunculin (Fig. 6I), and its normal asymmetric pattern (Fig. 6J) is abolished by exposure to Nocodozole (Fig. 6K). We conclude that cytoskeletal structure is required for the normal localization of both subunits along the animal-vegetal and LR axes.

Discussion

XKCNQ1 and XKCNE1 in Left-Right patterning

Pharmacological and molecular loss-of-function analyses implicate XKCNQ1 and XKCNE1 as obligate components of left-right patterning. Since co-transfection of ER-retention KCNE1 mutants is known to reduce cell surface expression of KCNQ1 [73], it is not yet known whether the randomizing effect of KCNE1 dominant negative constructs is due to reduction of the number of KCNQ1-KCNE1 complexes in the membrane, to reduction of

their activity on the cell surface, or both. Misexpression of XKCNE3 (Mirp2), a regulatory subunit in the KCNE family that opens KCNQ1 but suppresses ERG channels [63, 78], had no effect on asymmetry. Together with lack of a randomizing effect of constitutively open KCNQ1 mutants or of exposure to RL-3 [51], these data suggest that XKCNQ1 is already activated by default (since molecular or pharmacological activation does not randomize asymmetry).

XKCNQ1 and XKCNE1 proteins are present in embryos from prior to fertilization - long before the appearance of heart, neurons, or kidneys (tissues in which these channels are normally studied). Early embryos contain both maternal mRNA (Fig. 2, 4) and protein (Fig. 3, 5), and as previously described for several other ion transporters relevant to LR patterning [13, 15, 77], the distributions of mRNA and protein are not identical. While the possible role of differential degradation has not yet been explored, it is clear that one contributor to the specific localization of this channel is the cytoskeleton (Fig. 6), consistent with previous data implicating motor protein activity and oriented cytoskeletal tracks in asymmetric localization [19, 77], as well as with the known ability of adult mammalian cells to localize KCNQ1 along the apical-basal axis [79, 80].

Upstream components of the pathway: controls of XKCNQ1/XKCNE1 function

The expression of XKCNQ1 protein is asymmetrical, being localized to the right ventral cell (Fig. 3). While the plane of first cleavage can be experimentally repositioned [81, 82], in normal embryos the cleavage furrow usually corresponds to the future midline of the embryo [17, 18], and injection of one cell at the two-cell stage is routinely used to target half the embryo, allowing the contralateral half to serve as an internal control [83-85]. Thus, similarly to the V-ATPase [15] and H^+/K^+-ATPase [77] pumps, this early asymmetry of protein localization is predicted to align differences in ion flux (and thus, subsequent physiological asymmetries) with the prospective midline of LR asymmetry.

The asymmetric localization of XKCNQ1 and XKCNE1 requires cytoskeletal and organization (Fig. 6). This situation parallels the V-ATPase [15] and the H^+/K^+-ATPase [77], and indeed microtubule tracks are known to regulate a number of ion transporter systems in a variety of vertebrate cell types [74, 86-90]. Thus, the localization of this component of the early embryonic battery is dependent upon upstream intracellular polarity machinery.

Downstream components: how does XKCNQ1/XKCNE1 control asymmetry?

Prior work described models of mechanisms that transduce consistent asymmetries in bioelectric properties to subsequent steps canalized as asymmetric gene expression during gastrulation and neurulation [11, 21, 91, 92]. Asymmetric early distribution of the H^+/K^+-ATPase regulates left-right patterning by establishing differential membrane voltage gradients on the L and R sides [13, 21, 77] and indeed the importance of this pump for laterality has been documented in several vertebrate and invertebrate species [93-95]. Importantly however, this antiporter is electroneutral, since it swaps two positive charges in every cycle [96-98]. Our data on XKCNQ1 provide a possible resolution to the question of how the H^+/K^+-ATPase can control LR patterning (Fig. 7A).

XKCNQ1 contributes to resting potential [99, 100], and is a stabilizing component for transmembrane voltage in epithelial electrical polarity, including renal and gastrointestinal cells, as well as cells in the vestibule of the inner ear (all three of which are key sites for other bioelectrical systems necessary for LR patterning [11, 101, 102]). Thus, we suggest a similar function for this channel in the battery that exists on the ventral midline of *Xenopus* embryos (Fig. 7B): as in several mammalian tissues, where cellular K^+ ions exit through

KCNQ1 channels to recycle K^+ or maintain cell membrane potential [103], we propose that the function of XKCNQ1 channels in LR patterning is to provide an exit route for the potassium ions brought in by the H^+/K^+-ATPase, thus allowing this electroneutral antiporter to generate a change in membrane voltage by the net loss of positive ions in the right ventral blastomere. XKCNQ1 is an ideal candidate to function as part of the physiological module (including several channels and pumps) that generates the electrophoretic force for the known subsequent LR-asymmetric redistribution of small molecule morphogens through gap junctions [10]. Indeed, the potassium currents produced by KCNQ1 associated with members of the MiRP β subunits are activated by low extracellular pH [29, 104], a condition present at the right ventral blastomere's surface due to the action of the H^+/K^+-ATPase and V-ATPase pumps [13, 15]. Thus, the activity of XKCNQ1/XKCNE1 together with the two right-sided H^+ pumps results in a bioelectrical cassette that is conserved among embryonic LR patterning and adult gut/kidney/inner ear function.

This model makes specific predictions about the spatio-temporal function of XKCNQ1/XKCNE1. First, it requires that their roles in LR patterning occur during early cleavages. Indeed, XKCNE1 DNA does not induce heterotaxia as does XKCNE1 mRNA (although the DNA does cause other phenotypes such as hyperpigmentation, serving as a positive control for its activity; the analysis of this phenotype will be presented elsewhere). The fact that post-MBT expression of XKCNE1 is unable to affect laterality is consistent with this class of models [11] where the effects of K^+ modulation (and thus changes in V_{mem}) are paramount for LR patterning steps during cleavage stages in *Xenopus*. Similarly, a role in the LR physiological asymmetries requires that one or both of the components function differently on the L and R sides. Our data are consistent with this requirement, since we observed localization of XKCNQ1 maternal protein in the right ventral blastomere, precisely where the H^+/K^+-ATPase subunits are located.

What is the role of XKCNE1 in LR patterning? While the randomization by the dominant negative XKCNE1 construct (G46R, Table 2A) suggests that XKCNE1 itself is clearly necessary for normal LR patterning, the randomness of its localization with respect to the LR axis does not suggest straightforward models for how its presence contributes to consistent downstream asymmetry. It is possible that a balance (or net difference) of levels on the R and L sides is important, since global overexpression of both gain- and loss-of-function KCNE1 constructs both randomize asymmetry. This aspect remains puzzling, although this situation is not unprecedented in the field: localization of a kinesin-like protein that travels towards the "-" end of microtubules in Xenopus exhibits random asymmetry [77], as does the expression of Left-Right Dynein in the head-folds of the mouse [105]. Understanding the details of the early embryonic circuit will require probing in detail the roles of XKCNE1 and other accessory subunits. Nevertheless, the consistent asymmetry of the α subunit (XKCNQ1) fits into the known physiological circuit in a straight-forward way (Fig. 7C).

Evolutionary conservation of potassium channel roles in asymmetry

We have previously proposed that the LR axis is fundamentally an instance of epithelial planar polarity [11]. In this model, the frequent association between laterality defects and polycystic kidney disease [106-108] is due to the fundamental role of cellular polarization in kidney and embryonic cells [109], and in particular to the concordance of apical-basal and planar polarity systems that allows cytoskeleton-mediated alignment of bioelectrical (physiological) and morphological polarities [77]. Our functional and expression data on XKCNQ1 are consistent with this proposal, in light of the function and polarized localization of KCNQ1 in kidney cells [79, 110], its cooperation with the H^+/K^+-ATPase to control ion flux and pH in the gut [25-29], and its role in a number of epithelia [111, 112]. Indeed, KCNQ1 is asymmetrically localized along the basal-apical axis in kidney cells [80],

as are the other ion pumps that are now known to be important in LR patterning [11]. Importantly, KCNQ1 localization is controlled by the RAB11 GTPase [113], which is also implicated in the localization of components in the *Drosophila* wing and kidney cells [114-116] - classic examples of planar cell polarity.

The conservation of LR-relevant functions of XKCNQ1 and XKCNE1 to mammals is unclear. Genetic deletion of these loci in mice [103, 117] has not been reported to result in laterality defects. However, a human family was recently described, members of which exhibit both long QT syndrome and *situs inversus* [118]. While the specific mutation is not known, this finding supports the hypothesis that one of the LQT family of potassium channels in mammals plays a similar role in LR patterning as it does in *Xenopus*. Thus, it is possible that another channel compensates for this role in mouse knock-outs, suggesting that multiple (combinatorial) knock-out mice, or knock-ins with the dominant negative, will need to be generated in order to evaluate the role for this channel in mice. The clinical data do suggest the possibility that ion flux-dependent mechanisms of asymmetry may extend to human development, which in turn would significantly revise current models of the evolution of LR mechanisms [7, 109].

There is another fascinating link between KCNQ1 and human laterality. Non-conjoined monozygotic twins do not exhibit the visceral laterality defects that characterize conjoined twins, manifesting instead a subtle conservation of chirality (reviewed in [119]). "Bookend" or enantiomer twin pairs exhibit opposite directionality of markers such as hand preference, hair whorl direction, tooth patterns, unilateral eye and ear defects, cleft lip, cleft palate, supernumerary teeth, and even tumor locations and un-descended testicles [120-140]. Strikingly, it was recently shown that the human KCNQ1 gene is differentially imprinted in monozygotic twins [141, 142], suggesting a genetic entrypoint into the chirality-breaking events in human development. Since bioelectrical mechanisms of LR patterning appear to be well-conserved [109], and KCNQ is an evolutionarily-ancient family of channels, it is likely that an investigation of its roles in LR asymmetry of other model systems will reveal interesting additional information.

These data identify some very interesting and important areas for future investigation. We are pursuing the molecular motors (kinesins and dyneins) that provide the asymmetric localization of maternal XKCNQ1 proteins in early embryos. The exact contribution of XKCNE1 to XKCNQ1 function in L and R cells is an important piece of the puzzle, necessary to on-going efforts to quantitatively and mechanistically model early embryonic physiology of LR patterning [20]. KCNQ1 has a delayed repolarization, and association with KCNE1 slows the activation of KCNQ1 [31, 143]. It is unclear what such phenomena entail for embryonic patterning mechanisms that occur on the order of hours. Our current model of early physiology is steady-state, and the subtleties of kinetics will have to be incorporated into future efforts to understand the role of ion transport to developmental morphogenesis.

Acknowledgments

References

1. McCaig CD, Rajnicek AM, Song B, Zhao M. Controlling cell behavior electrically: Current views and future potential. Physiol Rev. 2005; 85:943–978. [PubMed: 15987799]

2. Levin M. Large-scale biophysics: Ion flows and regeneration. Trends Cell Biol. 2007; 17:262–271.

3. Cone CD. Unified theory on the basic mechanism of normal mitotic control and oncogenesis. J Theor Biol. 1971; 30:151–181. [PubMed: 5555269]

4. Levin M. Bioelectromagnetic patterning fields: Roles in embryonic development, regeneration, and neoplasm. Bioelectromagnetics. 2003; 24:295–315. [PubMed: 12820288]

5. Robinson KR, Messerli MA. Left/right, up/down: The role of endogenous electrical fields as directional signals in development, repair and invasion. Bioessays. 2003; 25:759–766. [PubMed: 12879446]

6. Borgens, R.; Robinson, K.; Vanable, J.; McGinnis, M. Electric fields in vertebrate repair. Alan R. Liss; New York: 1989.

7. Speder P, Petzoldt A, Suzanne M, Noselli S. Strategies to establish left/right asymmetry in vertebrates and invertebrates. Curr Opin Genet Dev. 2007

8. Neville, A. Animal asymmetry. Edward Arnold; London: 1976.

9. Raya A, Belmonte JC. Left-right asymmetry in the vertebrate embryo: From early information to higher-level integration. Nat Rev Genet. 2006; 7:283–293. [PubMed: 16543932]

10. Levin M. Left-right asymmetry in embryonic development: A comprehensive review. Mech Dev. 2005; 122:3–25. [PubMed: 15582774]

11. Levin M. Is the early left-right axis like a plant, a kidney, or a neuron? The integration of physiological signals in embryonic asymmetry. Birth Defects Res C Embryo Today. 2006; 78:191–223. [PubMed: 17061264]

12. Fukumoto T, Kema IP, Levin M. Serotonin signaling is a very early step in patterning of the left-right axis in chick and frog embryos. Curr Biol. 2005; 15:794–803. [PubMed: 15886096]

13. Levin M, Thorlin T, Robinson KR, Nogi T, Mercola M. Asymmetries in H^+/K^+-ATPase and cell membrane potentials comprise a very early step in left-right patterning. Cell. 2002; 111:77–89. [PubMed: 12372302]

14. Adams DS, Levin M. Inverse drug screens: A rapid and inexpensive method for implicating molecular targets. Genesis. 2006; 44:530–540. [PubMed: 17078061]

15. Adams DS, Robinson KR, Fukumoto T, Yuan S, Albertson RC, Yelick P, Kuo L, McSweeney M, Levin M. Early, H^+-V-ATPase-dependent proton flux is necessary for consistent left-right patterning of non-mammalian vertebrates. Development. 2006; 133:1657–1671. [PubMed: 16554361]

16. Aw, S.; Chen, I.; Scwappach, B.; Levin, M. The Katp channel is an early left-right patterning mechanism in chick and frog embryogenesis. in preparation

17. Masho R. Close correlation between the 1st cleavage plane and the body axis in early xenopus embryos. Dev Growth Differ. 1990; 32:57–64.

18. Klein SL. The first cleavage furrow demarcates the dorsal-ventral axis in xenopus embryos. Developmental Biology. 1987; 120:299–304. [PubMed: 3817297]

19. Qiu D, Cheng SM, Wozniak L, McSweeney M, Perrone E, Levin M. Localization and loss-of-function implicates ciliary proteins in early, cytoplasmic roles in left-right asymmetry. Dev Dyn. 2005; 234:176–189. [PubMed: 16059906]

20. Esser AT, Smith KC, Weaver JC, Levin M. Mathematical model of morphogen electrophoresis through gap junctions. Dev Dyn. 2006; 235:2144–2159. [PubMed: 16786594]

21. Raya A, Kawakami Y, Rodriguez-Esteban C, Ibanes M, Rasskin-Gutman D, Rodriguez-Leon J, Buscher D, Feijo JA, Izpisua Belmonte JC. Notch activity acts as a sensor for extracellular calcium during vertebrate left-right determination. Nature. 2004; 427:121–128. [PubMed: 14712268]

22. Sachs G, Shin JM, Briving C, Wallmark B, Hersey S. The pharmacology of the gastric acid pump: The H^+,K^+ ATPase. Annu Rev Pharmacol Toxicol. 1995; 35:277–305. [PubMed: 7598495]

23. Lambrecht NW, Yakubov I, Scott D, Sachs G. Identification of the k efflux channel coupled to the gastric H-K-ATPase during acid secretion. Physiol Genomics. 2005; 21:81–91. [PubMed: 15613615]

24. Wangemann P. K$^+$ cycling and the endocochlear potential. Hear Res. 2002; 165:1–9. [PubMed: 12031509]

25. Geibel JP. Role of potassium in acid secretion. World J Gastroenterol. 2005; 11:5259–5265. [PubMed: 16149129]

26. Dedek K. Colocalization of KCNQ1/KCNE channel subunits in the mouse gastrointestinal tract. Pflugers Arch. 2001; 442:896–902. [PubMed: 11680623]

27. Warth R. The multifaceted phenotype of the knockout mouse for the KCNE1 potassium channel gene. American Journal of Physiology - Regulatory Integrative & Comparative Physiology. 2002; 282:R639–648.

28. Lee MP, Ravenel JD, Hu RJ, Lustig LR, Tomaselli G, Berger RD, Brandenburg SA, Litzi TJ, Bunton TE, Limb C, Francis H, Gorelikow M, Gu H, Washington K, Argani P, Goldenring JR, Coffey RJ, Feinberg AP. Targeted disruption of the KVLQT1 gene causes deafness and gastric hyperplasia in mice. J Clin Invest. 2000; 106:1447–1455. [PubMed: 11120752]

29. Grahammer F, Herling AW, Lang HJ, Schmitt-Graff A, Wittekindt OH, Nitschke R, Bleich M, Barhanin J, Warth R. The cardiac K$^+$ channel KCNQ1 is essential for gastric acid secretion. Gastroenterology. 2001; 120:1363–1371. [PubMed: 11313306]

30. Bleich M, Warth R. The very small-conductance K$^+$ channel KVLQT1 and epithelial function. Pflugers Arch. 2000; 440:202–206. [PubMed: 10898519]

31. Lerche C, Seebohm G, Wagner CI, Scherer CR, Dehmelt L, Abitbol I, Gerlach U, Brendel J, Attali B, Busch AE. Molecular impact of mink on the enantiospecific block of I(ks) by chromanols. Br J Pharmacol. 2000; 131:1503–1506. [PubMed: 11139424]

32. Suessbrich H, Busch AE. The iks channel: Coassembly of Isk (mink) and KVLQT1 proteins. Rev Physiol Biochem Pharmacol. 1999; 137:191–226. [PubMed: 10207306]

33. Busch AE, Busch GL, Ford E, Suessbrich H, Lang HJ, Greger R, Kunzelmann K, Attali B, Stuhmer W. The role of the Isk protein in the specific pharmacological properties of the iks channel complex. Br J Pharmacol. 1997; 122:187–189. [PubMed: 9313924]

34. Wang Q, Curran ME, Splawski I, Burn TC, Millholland JM, VanRaay TJ, Shen J, Timothy KW, Vincent GM, de Jager T, Schwartz PJ, Toubin JA, Moss AJ, Atkinson DL, Landes GM, Connors TD, Keating MT. Positional cloning of a novel potassium channel gene: KVLQT1 mutations cause cardiac arrhythmias. Nat Genet. 1996; 12:17–23. [PubMed: 8528244]

35. Wollnik B, Schroeder BC, Kubisch C, Esperer HD, Wieacker P, Jentsch TJ. Pathophysiological mechanisms of dominant and recessive KVLQT1 K$^+$ channel mutations found in inherited cardiac arrhythmias. Hum Mol Genet. 1997; 6:1943–1949. [PubMed: 9302275]

36. Lande G, Demolombe S, Bammert A, Moorman A, Charpentier F, Escande D. Transgenic mice overexpressing human KVLQT1 dominant-negative isoform. Part ii: Pharmacological profile. Cardiovasc Res. 2001; 50:328–334. [PubMed: 11334836]

37. Unsold B, Kerst G, Brousos H, Hubner M, Schreiber R, Nitschke R, Greger R, Bleich M. KCNE1 reverses the response of the human K$^+$ channel kcnq1 to cytosolic ph changes and alters its pharmacology and sensitivity to temperature. Pflugers Arch. 2000; 441:368–378. [PubMed: 11211125]

38. Splawski I, Tristani-Firouzi M, Lehmann MH, Sanguinetti MC, Keating MT. Mutations in the hmink gene cause long QT syndrome and suppress Iks function. Nat Genet. 1997; 17:338–340. [PubMed: 9354802]

39. Casimiro MC, Knollmann BC, Ebert SN, Vary JC Jr. Greene AE, Franz MR, Grinberg A, Huang SP, Pfeifer K. Targeted disruption of the KCNQ1 gene produces a mouse model of Jervell and Lange-Nielsen syndrome. Proceedings of the National Academy of Sciences of the United States of America. 2001; 98:2526–2531. [PubMed: 11226272]

40. Nicolas M, Dememes D, Martin A, Kupershmidt S, Barhanin J. KCNQ1/KCNE1 potassium channels in mammalian vestibular dark cells. Hear Res. 2001; 153:132–145. [PubMed: 11223304]

41. Sive, HL.; Grainger, RM.; Harland, RM. Early development of xenopus laevis. Cold Spring Harbor Laboratory Press; New York: 2000.

42. Nieuwkoop, PD.; Faber, J. Normal table of *Xenopus laevis* (Daudin). ed 2nd. North-Holland Publishing Company; Amsterdam: 1967.

43. Harland, RM. In situ hybridization: An improved whole mount method for *xenopus* embryos. In: Kay, BK.; Peng, HB., editors. Xenopus laevis: Practical uses in cell and molecular biology. Vol. 36. Academic Press; San Diego: 1991. p. 685-695.

44. Levin M. A novel immunohistochemical method for evaluation of antibody specificity and detection of labile targets in biological tissue. Journal of Biochemical and Biophysical Methods. 2004; 58:85–96. [PubMed: 14597192]

45. Lesage F, Attali B, Lakey J, Honore E, Romey G, Faurobert E, Lazdunski M, Barhanin J. Are xenopus oocytes unique in displaying functional isk channel heterologous expression? Receptors Channels. 1993; 1:143–152. [PubMed: 8081718]

46. Bleich M, Briel M, Busch AE, Lang HJ, Gerlach U, Gogelein H, Greger R, Kunzelmann K. KVLQT channels are inhibited by the K^+ channel blocker 293b. Pflugers Arch. 1997; 434:499–501. [PubMed: 9211819]

47. Busch AE, Suessbrich H, Waldegger S, Sailer E, Greger R, Lang H, Lang F, Gibson KJ, Maylie JG. Inhibition of iks in guinea pig cardiac myocytes and guinea pig isk channels by the Chromanol 293B. Pflugers Arch. 1996; 432:1094–1096. [PubMed: 8781206]

48. Yang WP, Levesque PC, Little WA, Conder ML, Shalaby FY, Blanar MA. KVLQT1, a voltage-gated potassium channel responsible for human cardiac arrhythmias. Proc Natl Acad Sci U S A. 1997; 94:4017–4021. [PubMed: 9108097]

49. Lynch JJ Jr. Houle MS, Stump GL, Wallace AA, Gilberto DB, Jahansouz H, Smith GR, Tebben AJ, Liverton NJ, Selnick HG, Claremon DA, Billman GE. Antiarrhythmic efficacy of selective blockade of the cardiac slowly activating delayed rectifier current, I(ks), in canine models of malignant ischemic ventricular arrhythmia. Circulation. 1999; 100:1917–1922. [PubMed: 10545437]

50. Jensen HS, Callo K, Jespersen T, Jensen BS, Olesen SP. The KCNQ5 potassium channel from mouse: A broadly expressed m-current like potassium channel modulated by zinc, Ph, and volume changes. Brain Res Mol Brain Res. 2005; 139:52–62. [PubMed: 15963599]

51. Salata JJ, Jurkiewicz NK, Wang J, Evans BE, Orme HT, Sanguinetti MC. A novel benzodiazepine that activates cardiac slow delayed rectifier K^+ currents. Mol Pharmacol. 1998; 54:220–230. [PubMed: 9658209]

52. Scharf SR, Lieberman MB, Cande WZ. Determination of dorsoventral polarity in the Xenopus egg requires microtubules. Prog Clin Biol Res. 1986; 217B:345–348. [PubMed: 3749189]

53. Elinson RP, Rowning B. A transient array of parallel microtubules in frog eggs: Potential tracks for a cytoplasmic rotation that specifies the dorso-ventral axis. Dev Biol. 1988; 128:185–197. [PubMed: 3289985]

54. Chartrain I, Couturier A, Tassan JP. Cell-cycle-dependent cortical localization of peg3 protein kinase in Xenopus and human cells. Biol Cell. 2006; 98:253–263. [PubMed: 16159311]

55. Schatten G, Schatten H, Spector I, Cline C, Paweletz N, Simerly C, Petzelt C. Latrunculin inhibits the microfilament-mediated processes during fertilization, cleavage and early development in sea urchins and mice. Exp Cell Res. 1986; 166:191–208. [PubMed: 3743654]

56. Levin M, Mercola M. Gap junctions are involved in the early generation of left-right asymmetry. Dev Biol. 1998; 203:90–105. [PubMed: 9806775]

57. Danos MC, Yost HJ. Role of notochord in specification of cardiac left-right orientation in zebrafish and xenopus. Developmental Biology. 1996; 177:96–103. [PubMed: 8660880]

58. Sanguinetti M, Curran M, Zou A, Shen J, Spector P, Atkinson D, Keating M. Coassembly of K(V)LQT1 and Mink (isk) proteins to form cardiac I(ks) potassium channel. Nature. 1996; 384:80–83. [PubMed: 8900283]

59. Chen YH, Xu SJ, Bendahhou S, Wang XL, Wang Y, Xu WY, Jin HW, Sun H, Su XY, Zhuang QN, Yang YQ, Li YB, Liu Y, Xu HJ, Li XF, Ma N, Mou CP, Chen Z, Barhanin J, Huang W. KCNQ1 gain-of-function mutation in familial atrial fibrillation. Science. 2003; 299:251–254. [PubMed: 12522251]

60. Larsen LA, Fosdal I, Andersen PS, Kanters JK, Vuust J, Wettrell G, Christiansen M. Recessive romano-ward syndrome associated with compound heterozygosity for two mutations in the KVLQT1 gene. Eur J Hum Genet. 1999; 7:724–728. [PubMed: 10482963]

61. Splawski I, Shen J, Timothy KW, Lehmann MH, Priori S, Robinson JL, Moss AJ, Schwartz PJ, Towbin JA, Vincent GM, Keating MT. Spectrum of mutations in long-qt syndrome genes. KVLQT1, HERG, SCN5A, KCNE1, and KCNE2. Circulation. 2000; 102:1178–1185. [PubMed: 10973849]

62. Dahimene S, Alcolea S, Naud P, Jourdon P, Escande D, Brasseur R, Thomas A, Baro I, Merot J. The n-terminal juxtamembranous domain of KCNQ1 is critical for channel surface expression: Implications in the romano-ward LQT1 syndrome. Circ Res. 2006; 99:1076–1083. [PubMed: 17053194]

63. Anantharam A, Lewis A, Panaghie G, Gordon E, McCrossan ZA, Lerner DJ, Abbott GW. Rna interference reveals that endogenous Xenopus Mink-related peptides govern mammalian K^+ channel function in oocyte expression studies. J Biol Chem. 2003; 278:11739–11745. [PubMed: 12529362]

64. Ma L, Lin C, Teng S, Chai Y, Bahring R, Vardanyan V, Li L, Pongs O, Hui R. Characterization of a novel long qt syndrome mutation G52R-KCNE1 in a chinese family. Cardiovasc Res. 2003; 59:612–619. [PubMed: 14499862]

65. Lohr JL, Danos MC, Yost HJ. Left-right asymmetry of a nodal-related gene is regulated by dorsoanterior midline structures during *Xenopus* development. Dev Suppl. 1997; 124:1465–1472.

66. Hyatt BA, Lohr JL, Yost HJ. Initiation of vertebrate left-right axis formation by maternal vg1. Nature. 1996; 384:62–65. [PubMed: 8900277]

67. Fukumoto T, Blakely R, Levin M. Serotonin transporter function is an early step in left-right patterning in chick and frog embryos. Dev Neurosci. 2005; 27:349–363. [PubMed: 16280633]

68. Ocorr K, Reeves NL, Wessells RJ, Fink M, Chen HS, Akasaka T, Yasuda S, Metzger JM, Giles W, Posakony JW, Bodmer R. KCNQ potassium channel mutations cause cardiac arrhythmias in drosophila that mimic the effects of aging. Proc Natl Acad Sci U S A. 2007; 104:3943–3948. [PubMed: 17360457]

69. Ocorr K, Perrin L, Lim HY, Qian L, Wu X, Bodmer R. Genetic control of heart function and aging in drosophila. Trends Cardiovasc Med. 2007; 17:177–182. [PubMed: 17574126]

70. Wei AD, Butler A, Salkoff L. Kcnq-like potassium channels in caenorhabditis elegans. Conserved properties and modulation. J Biol Chem. 2005; 280:21337–21345. [PubMed: 15797864]

71. Wang Z, Tristani-Firouzi M, Xu Q, Lin M, Keating MT, Sanguinetti MC. Functional effects of mutations in KvLQT1 that cause long qt syndrome. J Cardiovasc Electrophysiol. 1999; 10:817–826. [PubMed: 10376919]

72. Bendahhou S, Marionneau C, Haurogne K, Larroque MM, Derand R, Szuts V, Escande D, Demolombe S, Barhanin J. In vitro molecular interactions and distribution of kcne family with KCNQ1 in the human heart. Cardiovasc Res. 2005; 67:529–538. [PubMed: 16039274]

73. Krumerman A, Gao X, Bian JS, Melman YF, Kagan A, McDonald TV. An lqt mutant mink alters KVLQT1 trafficking. Am J Physiol Cell Physiol. 2004; 286:C1453–1463. [PubMed: 14761891]

74. Verrey F, Groscurth P, Bolliger U. Cytoskeletal disruption in a6 kidney cells: Impact on endo/exocytosis and nacl transport regulation by antidiuretic hormone. J Membr Biol. 1995; 145:193–204. [PubMed: 7563021]

75. Cantiello HF. Role of the actin cytoskeleton on epithelial Na^+ channel regulation. Kidney Int. 1995; 48:970–984. [PubMed: 8569107]

76. Nelson WJ. Regulation of cell surface polarity in renal epithelia. Pediatr Nephrol. 1993; 7:599–604. [PubMed: 8251331]

77. Aw S, Adams DS, Qiu D, Levin M. H,K-ATPase protein localization and kir4.1 function reveal concordance of 3 axes during early determination of left-right asymmetry. Mechanisms of Development. 2007 in press.

78. Schroeder BC, Waldegger S, Fehr S, Bleich M, Warth R, Greger R, Jentsch TJ. A constitutively open potassium channel formed by kcnq1 and kcne3. Nature. 2000; 403:196–199. [PubMed: 10646604]

79. Jespersen T, Rasmussen HB, Grunnet M, Jensen HS, Angelo K, Dupuis DS, Vogel LK, Jorgensen NK, Klaerke DA, Olesen SP. Basolateral localisation of KCNQ1 potassium channels in mdck cells: Molecular identification of an n-terminal targeting motif. J Cell Sci. 2004; 117:4517–4526. [PubMed: 15316073]

80. Calloe K, Nielsen MS, Grunnet M, Schmitt N, Jorgensen NK. Kcnq channels are involved in the regulatory volume decrease response in primary neonatal rat cardiomyocytes. Biochim Biophys Acta. 2007; 1773:764–773. [PubMed: 17442416]

81. Danilchik MV, Black SD. The first cleavage plane and the embryonic axis are determined by separate mechanisms in *Xenopus laevis*. I. Independence in undisturbed embryos. Developmental Biology. 1988; 128:58–64. [PubMed: 2454855]

82. Black SD, Vincent JP. The first cleavage plane and the embryonic axis are determined by separate mechanisms in Xenopus laevis. Ii. Experimental dissociation by lateral compression of the egg. Developmental Biology. 1988; 128:65–71. [PubMed: 3384178]

83. Vize PD, Melton DA, Hemmati-Brivanlou A, Harland RM. Assays for gene function in developing *Xenopus* embryos. Methods in Cell Biology. 1991; 36:367–387. [PubMed: 1811145]

84. Warner AE, Guthrie SC, Gilula NB. Antibodies to gap-junctional protein selectively disrupt junctional communication in the early amphibian embryo. Nature. 1984; 311:127–131. [PubMed: 6088995]

85. Harvey RP, Melton DA. Microinjection of synthetic Xhox-1a homeobox mrna disrupts somite formation in developing xenopus embryos. Cell. 1988; 53:687–697. [PubMed: 2897242]

86. Li Q, Montalbetti N, Wu Y, Ramos A, Raychowdhury MK, Chen XZ, Cantiello HF. Polycystin-2 cation channel function is under the control of microtubular structures in primary cilia of renal epithelial cells. J Biol Chem. 2006; 281:37566–37575. [PubMed: 16950792]

87. Wu S, Chen H, Alexeyev MF, King JA, Moore TM, Stevens T, Balczon RD. Microtubule motors regulate isoc activation necessary to increase endothelial cell permeability. J Biol Chem. 2007

88. Rivera J, Chu PJ, Lewis TL Jr. Arnold DB. The role of kif5b in axonal localization of KV1 K(+) channels. Eur J Neurosci. 2007; 25:136–146. [PubMed: 17241275]

89. Wang Z, Eldstrom JR, Jantzi J, Moore ED, Fedida D. Increased focal kv4.2 channel expression at the plasma membrane is the result of actin depolymerization. Am J Physiol Heart Circ Physiol. 2004; 286:H749–759. [PubMed: 14551056]

90. Cantiello HF, Stow JL, Prat AG, Ausiello DA. Actin filaments regulate epithelial Na$^+$ channel activity. Am J Physiol. 1991; 261:C882–888. [PubMed: 1659214]

91. Levin M, Buznikov GA, Lauder JM. Of minds and embryos: Left-right asymmetry and the serotonergic controls of pre-neural morphogenesis. Dev Neurosci. 2006; 28:171–185. [PubMed: 16679764]

92. McGrath J, Somlo S, Makova S, Tian X, Brueckner M. Two populations of node monocilia initiate left-right asymmetry in the mouse. Cell. 2003; 114:61–73. [PubMed: 12859898]

93. Shimeld SM, Levin M. Evidence for the regulation of left-right asymmetry in *ciona intestinalis* by ion flux. Dev Dyn. 2006; 235:1543–1553. [PubMed: 16586445]

94. Hibino T, Ishii Y, Levin M, Nishino A. Ion flow regulates left-right asymmetry in sea urchin development. Dev Genes Evol. 2006; 216:265–276. [PubMed: 16534626]

95. Duboc V, Rottinger E, Lapraz F, Besnardeau L, Lepage T. Left-right asymmetry in the sea urchin embryo is regulated by nodal signaling on the right side. Dev Cell. 2005; 9:147–158. [PubMed: 15992548]

96. Wallmark B, Lorentzon P, Sachs G. The gastric H+,K(+)-ATPase. J Intern Med Suppl. 1990; 732:3–8. [PubMed: 2166525]

97. Rabon EC, Reuben MA. The mechanism and structure of the gastric H,K-ATPase. Annu Rev Physiol. 1990; 52:321–344. [PubMed: 2158765]

98. Doucet A. H+, K(+)-ATPase in the kidney: Localization and function in the nephron. Exp Nephrol. 1997; 5:271–276. [PubMed: 9259180]

99. Oliver D, Knipper M, Derst C, Fakler B. Resting potential and submembrane calcium concentration of inner hair cells in the isolated mouse cochlea are set by kcnq-type potassium channels. J Neurosci. 2003; 23:2141–2149. [PubMed: 12657673]

100. Brown BS, Yu SP. Modulation and genetic identification of the M channel. Prog Biophys Mol Biol. 2000; 73:135–166. [PubMed: 10958929]

101. Lecain E, Robert JC, Thomas A, Tran Ba Huy P. Gastric proton pump is expressed in the inner ear and choroid plexus of the rat. Hear Res. 2000; 149:147–154. [PubMed: 11033254]

102. Lang F, Vallon V, Knipper M, Wangemann P. Functional significance of channels and transporters expressed in the inner ear and the kidney. Am J Physiol Cell Physiol. 2007

103. Vallon V, Grahammer F, Volkl H, Sandu CD, Richter K, Rexhepaj R, Gerlach U, Rong Q, Pfeifer K, Lang F. Kcnq1-dependent transport in renal and gastrointestinal epithelia. Proc Natl Acad Sci U S A. 2005; 102:17864–17869. [PubMed: 16314573]

104. Heitzmann D, Koren V, Wagner M, Sterner C, Reichold M, Tegtmeier I, Volk T, Warth R. Kcne beta subunits determine ph sensitivity of kcnq1 potassium channels. Cell Physiol Biochem. 2007; 19:21–32. [PubMed: 17310097]

105. Supp DM, Brueckner M, Kuehn MR, Witte DP, Lowe LA, McGrath J, Corrales J, Potter SS. Targeted deletion of the atp binding domain of left-right dynein confirms its role in specifying development of left-right asymmetries. Dev Suppl. 1999; 126:5495–5504.

106. Murcia NS, Richards WG, Yoder BK, Mucenski ML, Dunlap JR, Woychik RP. The oak ridge polycystic kidney (ORPK) disease gene is required for left-right axis determination. Development. 2000; 127:2347–2355. [PubMed: 10804177]

107. Mochizuki T, Tsuchiya K, Yokoyama T. Molecular cloning of a gene for inversion of embryo turning (inv) with cystic kidney. Neph Dial Trans. 2002; 17:68–70.

108. Pennekamp P, Karcher C, Fischer A, Schweickert A, Skryabin B, Horst J, Blum M, Dworniczak B. The ion channel polycystin-2 is required for left-right axis determination in mice. Curr Biol. 2002; 12:938–943. [PubMed: 12062060]

109. Levin M, Palmer AR. Left-right patterning from the inside out: Widespread evidence for intracellular control. Bioessays. 2007; 29:271–287. [PubMed: 17295291]

110. Zheng W, Verlander JW, Lynch IJ, Cash M, Shao J, Stow LR, Cain BD, Weiner ID, Wall SM, Wingo CS. Cellular distribution of the potassium channel kcnq1 in normal mouse kidney. Am J Physiol Renal Physiol. 2007; 292:F456–466. [PubMed: 16896189]

111. Kunzelmann K, Hubner M, Schreiber R, Levy-Holzman R, Garty H, Bleich M, Warth R, Slavik M, von Hahn T, Greger R. Cloning and function of the rat colonic epithelial K+ channel KVLQT1. J Membr Biol. 2001; 179:155–164. [PubMed: 11220365]

112. Bleich M, Warth R. The very small-conductance K+ channel KVLQT1 and epithelial function. Pflugers Arch. 2000; 440:202–206. [PubMed: 10898519]

113. Seebohm G, Strutz-Seebohm N, Birkin R, Dell G, Bucci C, Spinosa MR, Baltaev R, Mack AF, Korniychuk G, Choudhury A, Marks D, Pagano RE, Attali B, Pfeufer A, Kass RS, Sanguinetti MC, Tavare JM, Lang F. Regulation of endocytic recycling of KCNQ1/KCNE1 potassium channels. Circ Res. 2007; 100:686–692. [PubMed: 17293474]

114. Li BX, Satoh AK, Ready DF. Myosin v, rab11, and drip11 direct apical secretion and cellular morphogenesis in developing drosophila photoreceptors. J Cell Biol. 2007; 177:659–669. [PubMed: 17517962]

115. Babbey CM, Ahktar N, Wang E, Chen CC, Grant BD, Dunn KW. Rab10 regulates membrane transport through early endosomes of polarized madin-darby canine kidney cells. Mol Biol Cell. 2006; 17:3156–3175. [PubMed: 16641372]

116. Classen AK, Anderson KI, Marois E, Eaton S. Hexagonal packing of drosophila wing epithelial cells by the planar cell polarity pathway. Dev Cell. 2005; 9:805–817. [PubMed: 16326392]

117. Warth R, Garcia Alzamora M, Kim JK, Zdebik A, Nitschke R, Bleich M, Gerlach U, Barhanin J, Kim SJ. The role of KCNQ1/KCNE1 K(+) channels in intestine and pancreas: Lessons from the kcne1 knockout mouse. Pflugers Arch. 2002; 443:822–828. [PubMed: 11889581]

118. Corcos AP, Tzivoni D, Medina A. Long QT syndrome and complete situs inversus. Preliminary report of a family. Cardiology. 1989; 76:228–233. [PubMed: 2776143]

119. Levin M. Twinning and embryonic left-right asymmetry. Laterality. 1999; 4:197–208. [PubMed: 15513114]

120. Newman, H.; Freeman, F.; Holzinger, K. Twins: A study of heredity and environment. University of Chicago Press; Chicago: 1937.

121. Gedda L, Brenci G, Franceschetti A, Talone C, Ziparo R. Study of mirror imaging in twins. Prog Clin Biol Res. 1981; 69A:167–168. [PubMed: 7301887]

122. Carton A, Rees RT. Mirror image dental anomalies in identical twins. Br Dent J. 1987; 162:193–194. [PubMed: 3470026]

123. Yager J. Asymmetry in monozygotic twins. American Journal of Psychiatry. 1984; 141:719–720. [PubMed: 6538763]

124. Beere D, Hargreaves J, Sperber G, Cleaton-Jones P. Mirror image supplemental primary incisor teeth in twins: Case report and review. Pediatr Dent. 1990; 12:390–392. [PubMed: 2087414]

125. Townsend G, Richards L. Twins and twinning, dentists and dentistry. Aust Dent J. 1990; 35:317–327. [PubMed: 2099767]

126. Morison D, Reyes C, Skorodin M. Mirror-image tumors in mirror-image twins. Chest. 1994; 106:608–610. [PubMed: 7774348]

127. Cidis MB, Warshowsky JH, Goldrich SG, Meltzer CC. Mirror-image optic nerve dysplasia with associated anisometropia in identical twins. J Am Optom Assoc. 1997; 68:325–329. [PubMed: 9170799]

128. Morini F, Ilari M, Casati A, Pisera A, Oriolo L, Cozzi DA. Posterior urethral valves and mirror image anomalies in monozygotic twins. Am J Med Genet. 2002; 111:210–212. [PubMed: 12210353]

129. Sperber GH, Machin GA, Bamforth FJ. Mirror-image dental fusion and discordance in monozygotic twins. Am J Med Genet. 1994; 51:41–45. [PubMed: 8030668]

130. Mensing CA. Mirror-image twins. Northwest Dent. 1983; 62:41–42. [PubMed: 6581474]

131. Schneider PE. Mirror-image twins with geminated incisors. Report of a case. Quintessence Int. 1985; 16:429–431. [PubMed: 3862167]

132. West VC. Case reports. Mirror image twins. Australian Orthodontic Journal. 1985; 9:243. [PubMed: 3870085]

133. Sommer IE, Ramsey NF, Mandl RC, Kahn RS. Language lateralization in monozygotic twin pairs concordant and discordant for handedness. Brain. 2002; 125:2710–2718. [PubMed: 12429598]

134. Sommer I, Ramsey N, Bouma A, Kahn R. Cerebral mirror-imaging in a monozygotic twin. Lancet. 1999; 354:1445–1446. [PubMed: 10543677]

135. Okamoto F, Nonoyama T, Hommura S. Mirror image myopic anisometropia in two pairs of monozygotic twins. Ophthalmologica. 2001; 215:435–438. [PubMed: 11741111]

136. Satoh K, Shibata Y, Tokushige H, Onizuka T. A mirror image of the first and second branchial arch syndrome associated with cleft lip and palate in monozygotic twins. Br J Plast Surg. 1995; 48:601–605. [PubMed: 8548164]

137. Lauterbach CE. Studies in twin resemblance. Genetics. 1925; 10:525–568. [PubMed: 17246288]

138. Rife DC. Handedness, with special reference to twins. Genetics. 1940; 25:178–186. [PubMed: 17246963]

139. Rife DC. Genetic studies of monozygotic twins, iii: Mirror-imaging. J Hered. 1933; 24:443–446.

140. Potter RH, Nance WE. A twin study of dental dimension. I. Discordance, asymmetry, and mirror imagery. American Journal of Physical Anthropology. 1976; 44:391–395. [PubMed: 945700]

141. Weksberg R, Shuman C, Caluseriu O, Smith AC, Fei YL, Nishikawa J, Stockley TL, Best L, Chitayat D, Olney A, Ives E, Schneider A, Bestor TH, Li M, Sadowski P, Squire J. Discordant kcnq1ot1 imprinting in sets of monozygotic twins discordant for beckwith-wiedemann syndrome. Hum Mol Genet. 2002; 11:1317–1325. [PubMed: 12019213]

142. Xin Z, Soejima H, Higashimoto K, Yatsuki H, Zhu X, Satoh Y, Masaki Z, Kaneko Y, Jinno Y, Fukuzawa R, Hata J, Mukai T. A novel imprinted gene, KCNQ1dn, within the wt2 critical region of human chromosome 11p15.5 and its reduced expression in Wilms' tumors. Journal of Biochemistry. 2000; 128:847–853. [PubMed: 11056398]

143. Abbott GW, Goldstein SA. Potassium channel subunits encoded by the kcne gene family: Physiology and pathophysiology of the mink-related peptides (mirps). Mol Interv. 2001; 1:95–107. [PubMed: 14993329]

144. Chouabe C, Neyroud N, Guicheney P, Lazdunski M, Romey G, Barhanin J. Properties of KVLQT1 K+ channel mutations in romano-ward and jervell and lange-nielsen inherited cardiac arrhythmias. Embo J. 1997; 16:5472–5479. [PubMed: 9312006]

145. Anantharam A, Abbott GW. Does herg coassemble with a beta subunit? Evidence for roles of mink and Mirp1. Novartis Found Symp. 2005; 266:100–112. discussion 112-107, 155-108. [PubMed: 16050264]

146. Cho HC, Tsushima RG, Nguyen TT, Guy HR, Backx PH. Two critical cysteine residues implicated in disulfide bond formation and proper folding of Kir2.1. Biochem. 2000; 39:4649–4657. [PubMed: 10769120]

147. Levin M. The embryonic origins of left-right asymmetry. Crit Rev Oral Biol Med. 2004; 15:197–206. [PubMed: 15284185]
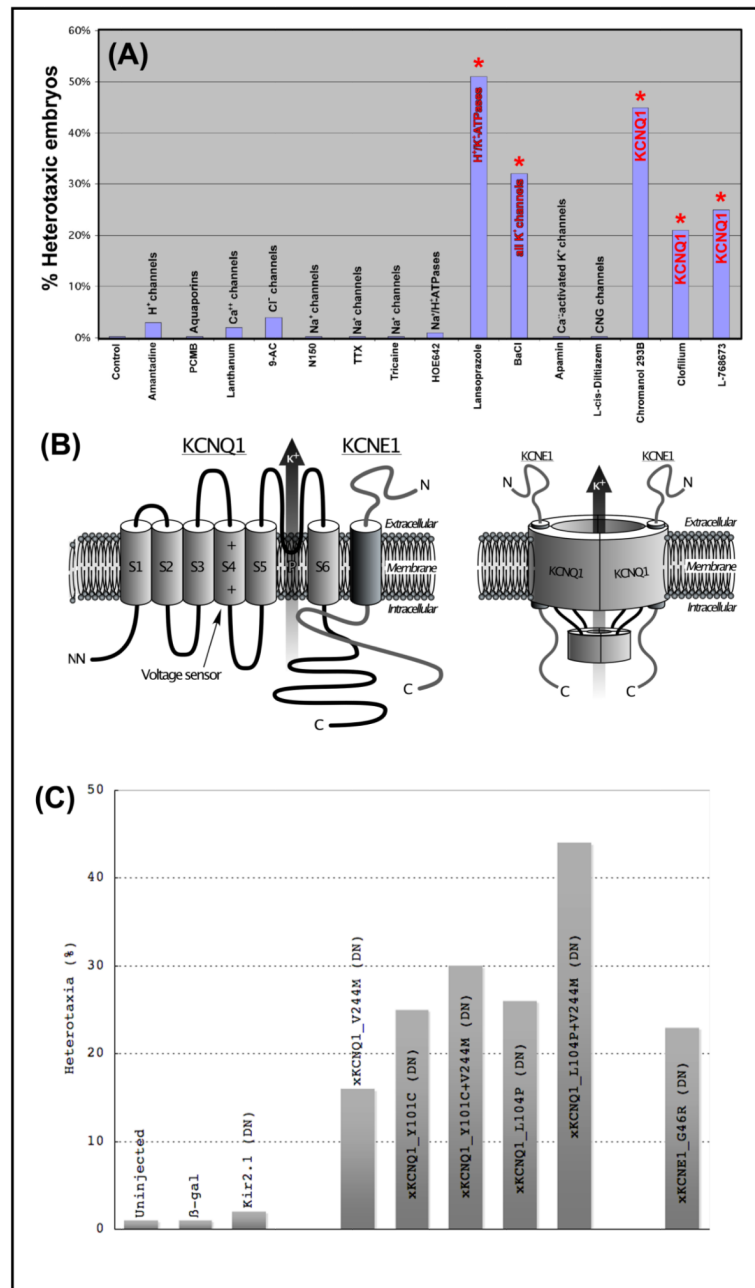
Fig. 1.
A drug screen implicates XKCNQ1 as a high-priority candidate in LR asymmetry. (A) Summary of drug screen data demonstrating that inhibitors targeting XKCNQ1, or the previously-characterized H^+/K^+-ATPase (positive control), specifically induce significant levels of the independent *situs* of the heart, gut, and gall-bladder, whereas a variety of other blockers do not. Embryos were exposed to each compound immediately after fertilization and washed out into 0.1X MMR medium at stage 8. They were scored for heterotaxia at st. 44. The doses uses were as follows: HOE642 2.6 mM, spermidine 95 μM, Lanthanum 100 μM, 9-anthracenecarboxylic acid 67 μM, tetrodotoxin 31 μM, MS-222 1.9 μM, Apamin 6.1 μM. The concentrations reported in the literature for these reagents derive largely from the characterization of mammalian channels. Since the *Xenopus* versions may be somewhat

divergent in sequence (and thus have a structure that may not bind the blocker with the same avidity), somewhat greater doses were utilized to reduce the probability of false negatives and to increase the validity of the negative results (which is the case for most of the reagents we explored). (B) KCNQ1 (also known as KvLQT-1) is a 6-transmembrane member of the K^+ channel family (schematic modeled on those in [144, 145]). When co-assembled with KCNE1 (also known as minK), it forms the "slow delayed rectifier" or I_{ks} channel [30]. KCNQ1 has different pharmacological profiles depending on whether it is associated with KCNE1 [32, 33]. (C) Histogram summarizing the effects of misexpression of molecular dominant negative constructs (injected at 1-cell stage, and analyzed at st. 44 for *situs* of heart, gut, and gall-bladder, Table 2A). Microinjections of control mRNAs, including β-gal and a Kir2.1 dominant negative [146], has no significant effect on laterality, while misexpression of dominant negative mutations of XKCNE1 or XKCNQ1 induced significant incidence of heterotaxia. Two of the XKCNQ1 mutations (recovered in human cases of long QT syndrome, labeled as "L104V+V244M") were additive and induced a higher incidence of laterality phenotype than either mutant alone.
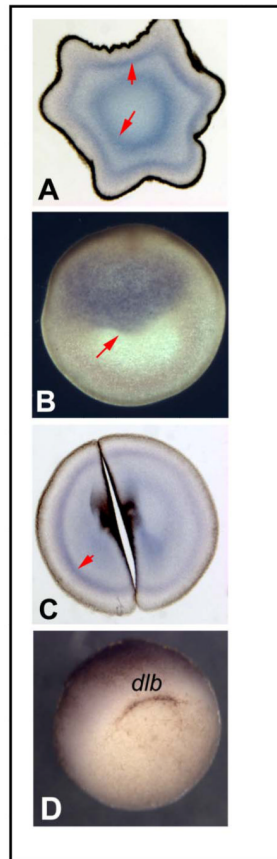
Fig. 2.
Expression of XKCNQ1 mRNA. *In situ* hybridization was performed on embryos at various stages with an antisense probe to native *Xenopus* KCNQ1. Panels A and C show JB4 sections made after hybridization in wholemount, while section B shows hybridization made directly on a gelatin-albumin section as described in [44]. (A) Eggs sectioned perpendicularly to the animal-vegetal (AV) axis contain two concentric domains of maternal XKCNQ1 mRNA. (B) Sections made through a fertilized egg along the animal-vegetal axis revealed the presence of maternal mRNA in the animal half of the egg. (C) Embryos at the 2-cell stage sectioned perpendicular to the AV axis reveal maternal mRNA in both blastomeres. (D) Gastrulating embryos show no expression in the organizer or elsewhere.
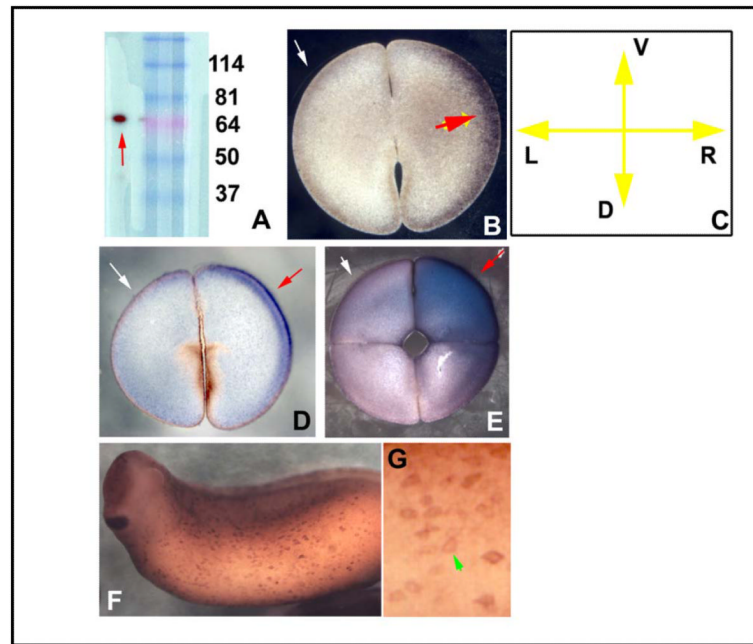
Fig. 3.
Localization of XKCNQ1 protein. (A) Western blotting of frog embryo extract against the XKCNQ1 antibody revealed a single clean band of the expected size. This antibody was then used on gelatin-albumin sections [44] of early embryos in alkaline-phosphatase immunohistochemistry. Embryos at the 2-cell stage sectioned perpendicular to the AV axis exhibited LR-asymmetric localization at the cell membrane and the immediately adjacent cortex (B). Section orientation is schematized in panel C (V=ventral, D=dorsal, L=left, R=right). At the late 2-cell stage, the stain became more localized to the ventral half of the cell (D) and by the 4-cell stage this could be oriented such that the positive cell was the right ventral one (E). Staining in wholemount the epidermis of the tailbud embryo (F) revealed signal in a subset of the skin cells, which in closeup exhibited the cell-membrane localization (green arrowhead) predicted for an ion channel subunit (G).

Fig. 4.
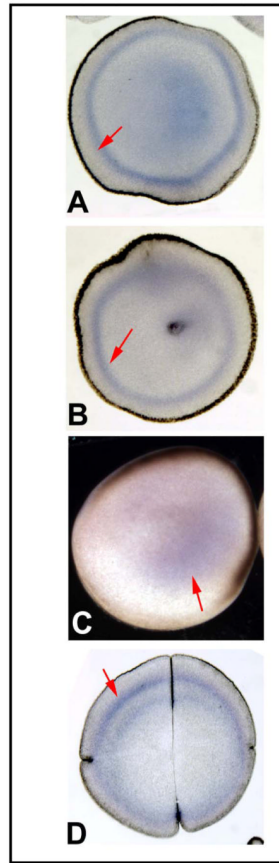Expression of XKCNE1 mRNA. Sections through mature oocytes (A) and fertilized eggs (B) both revealed a circumferential pattern of maternal XKCNE1 mRNA. *In situ* hybridization performed on sections taken through the animal-vegetal axis of fertilized eggs revealed maternal mRNA in the middle portion of the cell (C). During subsequent cleavages, mRNA was detected in the blastomeres in a thin band below the cell cortex (D).
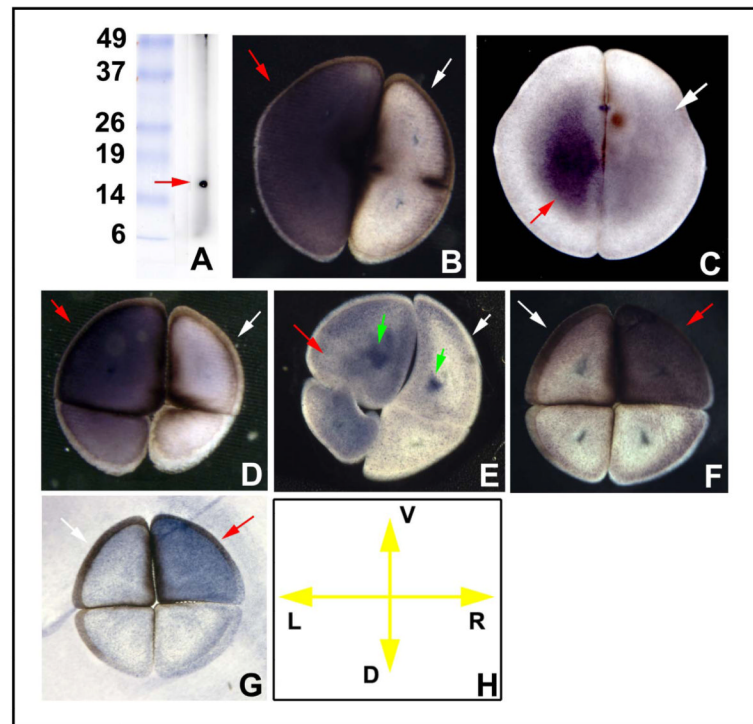
Fig. 5.
Localization of XKCNE1 protein. (A) Western blotting of frog embryo extract against the KCNE1 antibody revealed a single band of the predicted size. Immunoshitochemistry on gelatin-albumin sections taken perpendicular to the AV axis revealed asymmetric staining, which varied among left-handed blastomeres evenly-filled with signal (B) and more vegetal sections which exhibited staining mainly in the center (C), shown to be ventral at the 4-cell stage (D). In more vegetal sections at the 4-cell stage, central spots were observed (E), and in an equal number of embryos, it was the right ventral cell that was positive (F,G). Section orientation is schematized in panel H (V=ventral, D=dorsal, L=left, R=right). Red arrows indicate positive signal; white arrows indicate lack of signal.
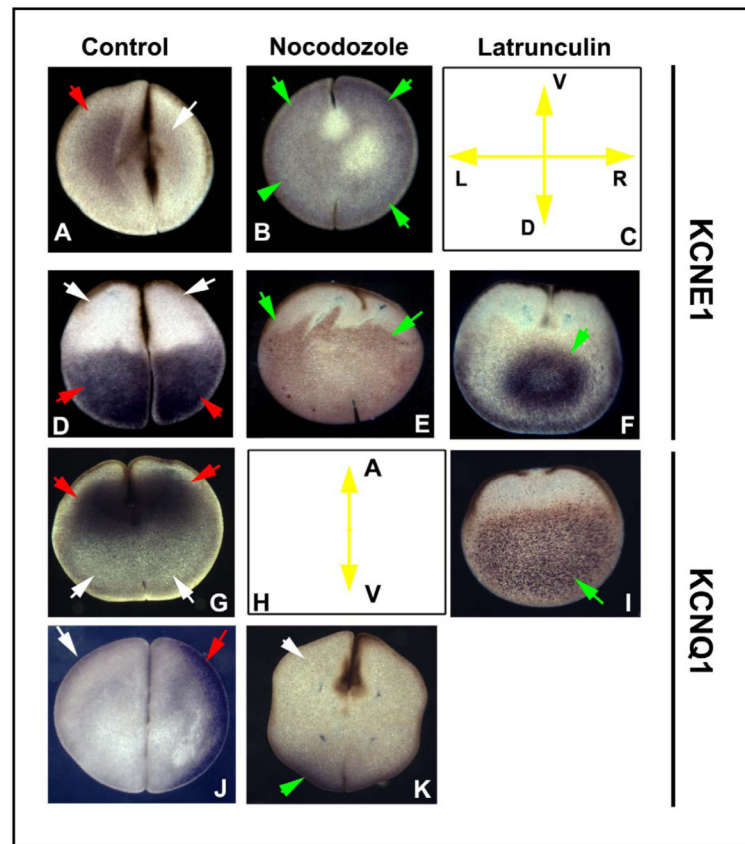
Fig. 6.
Localization of XKCNE1 and XKCNQ1 depends on microtubule and actin cytoskeleton. Embryos were treated with disruptors of microtubule organization (Nocodozole) or of actin organization (Latrunculin) for 2 hours after fertilization, and the embryos were fixed, sectioned in different planes, and processed for immunohistochemistry with KCNE1 and XKCNQ1 antibodies. The normal LR-asymmetric localization of XKCNE1 protein is altered from an asymmetric pattern (A) to a symmetrical one when embryos are exposed to Nocodozole (B). Section orientation is schematized in (C) (V=ventral, D=dorsal, L=left, R=right). Along the AV axis, the normal vegetal localization of XKCNE1 (D) is expanded towards the animal pole by disruption of the microtubules (E) and coalesced into a more restricted pattern in the center of the cell by disruption of the actin cytoskeleton (F). Likewise, the normal animal-pole localization of XKCNQ1 (G), schematized in panel H, is converted to a vegetal localization by Latrunculin (I), and the normal LR-asymmetric localization (J) is converted into a dorsal pattern (K) by exposure to Nocodozole. The cleavage furrows in some panels (e.g. F, I, and E) are not apparent even though all embryos are the same age because disruption of cytoskeleton also perturbs cytokinesis. Red arrows indicate positive signal; white arrows indicate lack of signal; green arrows indicate signal that is in an aberrant location.
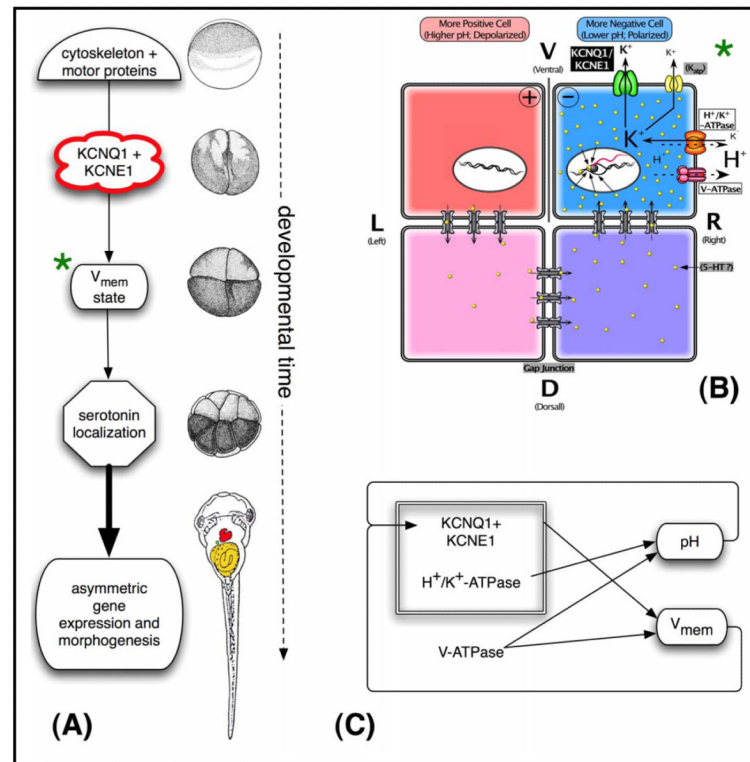
Fig. 7.
A model of XKCNQ1/XKCNE1 function in LR patterning. (A) Functional steps and a timeline of representative *Xenopus* stages of a model integrating the data on XKCNQ1/XKCNE1 function into known mechanisms of LR patterning [7, 10]. We propose that the early localization of XKCNQ1 and XKCNE1 is determined by cytoskeleton-dependent intracellular transport, analogously to other LR-relevant ion transporters [15, 77]. The asymmetric localization of this channel complex results in differential ion transport on the Left and Right sides, contributing to membrane voltage stage in ventral blastomeres across the midline [13, 15]. This physiological asymmetry controls downstream laterality pathways through serotonin localization [20, 91] or other transducers such as calcium signaling [21, 92], ultimately leading to the correct morphogenesis of the heart and viscera. Right column shows approximate *Xenopus* developmental stages corresponding to each event (diagrams taken from [42]). (B) A more detailed model of the module (marked with green asterisk) in panel A, whereby XKCNQ1 contributes to the asymmetries in membrane voltage during early cleavages. Specifically, we propose that this potassium channel (and perhaps others) provides an exit path for the extra K^+ ions brought in by the H^+/K^+-ATPase, thus (analogously to their cooperation in the mammalian gut) allowing this electroneutral pump to generate a voltage gradient by the net loss of positive charges. As we proposed previously [11, 147], asymmetries in XKCNQ1 in ventral cells across the LR midline can contribute to the electrophoretic force responsible for the asymmetric distribution of small molecule signals across gap junctional paths, resulting in asymmetric gene expression. (C) Complex feedback circuits control the bioelectrical state of the early blastomeres. The V-ATPase directly produces a pH gradient and helps set the membrane voltage gradient. The H^+/K^+-ATPase, in concert with potassium channels like KCNQ1, also contributes to transmembrane potential. Importantly, the KCNQ1/KCNE1 channel is sensitive to both membrane voltage and pH. Thus, this system may exhibit interesting and possibly non-linear dynamics over both the short-term and steady-state time scales, necessitating quantitative modeling in future work.

Table 1

drug screen data implicate KCNQ1. Legend:A comprehensive inverse drug screen was performed as previously described [14], with specific reversals of one or more of the heart, gut, or gall bladder being scored as an instance of heterotaxia. Most drug inhibitors targeting ion transporters had no effect on LR asymmetry, but two pumps had previously been implicated; see [13, 15] for primary data identifying the numerous ion transporters that are not implicated in LR patterning, as further negative controls. While embryos treated with vehicle only exhibited the normal 1% background of heterotaxia, exposure from fertilization to st. 8 to 1 mg/ml barium chloride resulted in a significant degree of randomization (68%, p<<0.01). Similarly, exposure to the KCNQ blockers Chromanol293B (300 μM) [46, 47], Clofilium tosylate (100 μM) [48], L-768673 (90 μM) [49], and Linopiridine (5 mM) [50] induce significant rates of heterotaxia.

Affected	Control Embryos		Chromanol 293B		Clofilium		L-768673		Linopiridine		BaCl	
Drug target:			KCNQ1		KCNQ1		KCNQ1		KCNQ1		general K+ channel blocker	
heart			10	20%	2	22%	7	54%	0	0%	13	27%
stomach			3	6%	0	0%	0	0%	2	18%	4	8%
gall bladder			0	0%	0	0%	0	0%	0	0%	2	4%
heart and stomach			0	0%	0	0%	0	0%	0	0%	0	0%
heart and gall bladder			0	0%	0	0%	0	0%	1	9%	1	2%
stomach & gall bladder			17	35%	4	44%	1	8%	2	18%	5	10%
heart, stomach, and gall bladder			19	39%	3	33%	5	38%	6	55%	24	49%
totals:			49		9		13		11		49	
Situs solitus (wild-type)	515	99%	59	55%	33	79%	38	75%	29	73%	102	68%
Heterotaxia:	5	1%	49	45%	9	21%	13	25%	11	28%	49	32%
total:	520		108		42		51		40		151	
χ^2			218.8		58.9		83.7		84.9		152.6	
p value			$1.7 \cdot 10^{-49}$		$1.7 \cdot 10^{-14}$		$5.8 \cdot 10^{-20}$		$3.1 \cdot 10^{-20}$		$4.8 \cdot 10^{-35}$	

Table 2A

Molecular loss-of-function confirms requirement for KCNQ1 /KCNE1 in LR patterning. Legend:To validate the pharmacological implication of KCNQ1 using gene-specific molecular reagents, embryos at the 1-cell stage were injected with synthetic mRNA encoding dominant-negative XKCNQ1 proteins. While embryos injected with β-gal mRNA (negative control) only exhibited the normal background of heterotaxia, misexpression of the mutant V244M [71], L104P [62], and the double mutant L104P+V244M all caused significant levels of heterotaxia (p<<0.01), as did the dominant negative mutant of XKCNE1, G46R [64].

Affected	ß-gal		V244M		L104P		L104P + V244M		G46R	
	Neg. ctrl		XKCNQ1 dominant negatives				XKCNQ1 dominant negatives		XKCNE1 dominant negative	
heart	0	0%	53	26%	16	32%	34	33%	15	16%
stomach	0	0%	12	6%	4	8%	8	8%	3	3%
gall bladder	0	0%	1	0%	1	2%	0	0%	0	0%
heart and stomach	0	0%	2	1%	0	0%	0	0%	0	0%
heart and gall bladder	0	0%	5	2%	0	0%	5	5%	0	0%
stomach & gall bladder	1	50%	54	27%	16	32%	27	26%	32	35%
heart, stomach, and gall bladder	1	50%	74	37%	13	26%	28	27%	41	45%
totals:	2		201		50		102		91	
Situs solitus (wild-type)	844	100%	1057	84%	147	75%	128	56%	297	77%
Heterotaxia:	2	0%	201	16%	50	25%	102	44%	91	23%
total:	846		1258		197		230		388	
χ^2			142.0		208.0		398.0		202.4	
p value			$9.82 \cdot 10^{-33}$		$3.77 \cdot 10^{-47}$		$1.52 \cdot 10^{-88}$		$6.11 \cdot 10^{-46}$	

Table 2B

Molecular gain-of-function demonstrates that over-expression of KCNE1 randomizes asymmetry. Legend:Embryos at the 1-cell stage were injected with synthetic mRNA or DNA encoding wild-type *Xenopus* laevis KCNE1 protein. Embryos injected with β-gal mRNA (negative control) did not exhibit high levels of laterality defects; neither did XKCNE1 DNA, even though it was efficiently transcribed and translated (the embryos did exhibit a hyperpigmentation phenotype of 20%). Unlike DNA, which in *Xenopus* produces mRNA and protein only after st. 8, misexpression of XKCNE1 mRNA (which begins translation immediately upon injection) caused highly significant heterotaxia (p<<0.01).

Affected	β-gal		XKCNE1 mRNA		XKCNE1 DNA	
	Neg. ctrl		KCNE1 wild-type protein by 4-cell stage		KCNE1 wild-type protein by st. 9	
heart	0	0%	42	19%	1	14%
stomach	0	0%	3	1%	1	14%
gall bladder	0	0%	3	1%	0	0%
heart and stomach	0	0%	1	0%	0	0%
heart and gall bladder	0	0%	9	4%	1	14%
stomach & gall bladder	1	50%	60	28%	1	14%
heart, stomach, and gall bladder	1	50%	99	46%	3	43%
totals:	2		217		7	
Situs solitus (wild-type)	844	100%	958	82%	193	96.5%
Heterotaxia:	2	0%	217	18%	7	3.5%
total:	846		1175		200	
χ^2			167		17	
p value			$2.8 \cdot 10^{-38}$		0.000047	